Journal of Pharmaceutical Analysis 9 (2019) 423–430

Contents lists available at ScienceDirect

Journal of Pharmaceutical Analysis

journal homepage: www.elsevier.com/locate/jpa

Original Article

Study on degradation kinetics of epalrestat in aqueous solutions and characterization of its major degradation products under stress degradation conditions by UHPLC-PDA-MS/MS

Hong Sun [a], Suyan Liu [b], Xun Gao [b], Zhili Xiong [b], Zhonggui He [b], Longshan Zhao [b,*]

[a] Shanxi Biosample Analysis Center, Shanxi Health Vocational College, No. 100, Wenjin Street, Yuci District, Jinzhong 030619, PR China
[b] School of Pharmacy, Shenyang Pharmaceutical University, No. 103, Wenhua Road, Shenyang 110016, PR China

ARTICLE INFO

Article history:
Received 14 December 2017
Received in revised form
23 July 2018
Accepted 9 August 2018
Available online 15 August 2018

Keywords:
Epalrestat
RP-HPLC
Degradation kinetics
UHPLC-PDA-MS/MS
Degradation products

ABSTRACT

Drug stability is closely related to drug safety and needs to be considered in the process of drug production, package and storage. To investigate the stability of epalrestat, a carboxylic acid derivative, a reversed-phase high-performance liquid chromatography (RP-HPLC) method was developed in this study and applied to analyzing the degradation kinetics of epalrestat in aqueous solutions in various conditions, such as different pH, temperatures, ionic strengths, oxidation and irradiation. The calibration curve was $A = 1.6 \times 10^5C–1.3 \times 10^3$ ($r = 0.999$) with the liner range of 0.5–24 μg/mL, the intra-day and inter-day precision was less than 2.0%, as was the repeatability. The average accuracy for different concentrations was more than 98.5%, indicating that perfect recoveries were achieved. Degradation kinetic parameters such as degradation rate constants (k), activation energy (Ea) and shelf life ($t_{0.9}$) under different conditions were calculated and discussed. The results indicated that the degradation behavior of epalrestat was pH-dependent and the stability of epalrestat decreased with the rised irradiation and ionic strength; however, it was more stable in neutral and alkaline conditions as well as lower temperatures. The results showed that the degradation kinetics of epalrestat followed first-order reaction kinetics. Furthermore, the degradation products of epalrestat under stress conditions were identified by UHPLC-PDA-MS/MS, with seven degradation products being detected and four of them being tentatively identified.

1. Introduction

Epalrestat (5-[(1*Z*,2*E*)− 2-methyl-3-phenylpropenylidene]-4-oxo-2-thioxo-3-thiazolidie acetic acid), which is approved for human use in Japan, is a carboxylic acid derivative and is currently available for the treatment of diabetic peripheral neuropathy [1–7]. Diabetic peripheral neuropathy is one of the most common long-term complications in diabetic patients [8–10]. Modern pharmaco-studies have indicated that epalrestat reduces sorbitol accumulation in the sciatic nerve, erythrocytes, and ocular tissues in animals, and erythrocytes in humans [11,12]. Epalrestat is increasingly applied in the clinic as it is presently the only aldose reductase inhibitor with less severe side effects [13–18]. Numerous reports have been published investigating related substances, the content assay by RP-HPLC [19,20]. Two methods were described on the quantitative determination in bulk and pharmaceutical dosage forms [21,22]. An HPLC method was established for the determination of its stereoisomers [23]. In addition, two LC-MS/MS methods [4,24], three HPLC methods [25–27], and an HPTLC method [28] were developed and validated for the quantification of epalrestat in biological samples.

Changes to properties of epalrestat in aqueous solution under the influence of various environmental factors over time are also of great importance and merit further study, as do storage conditions. Moreover, the degradation products may compromise therapeutic efficacy and cause toxic or unexpected severe side effects in patients [29–32]. Epalrestat exists as yellow to orange crystals or as crystalline powder and gradually fades and decomposes on exposure to light. The stability of epalrestat decreases on exposure to light, especially in aqueous solution. Furthermore, benzene, conjugated dienes, and thiazole ring that may organize toxic structures under stress degradation conditions are present in the structure of epalrestat. Nevertheless, in the cases above, there is no report on the study of its stability and no identification of its degradation products. The International Conference on Harmonization (ICH) guidelines suggest that stress degradation studies are carried out on a compound to establish its inherent stability characteristics not only to understand the stability of drug molecules but also to identify degradation products.

Peer review under the responsibility of Xi'an Jiaotong University.
* Corresponding author.
E-mail address: longshanzhao@163.com (L. Zhao).

https://doi.org/10.1016/j.jpha.2018.08.002

Therefore, studies on the degradation of epalrestat and identification of degradation products are essential.

This study aimed to analyze the degradation kinetics of epalrestat in aqueous solutions under the conditions of varying pH, temperature, ionic strength, oxidation and irradiation and to identify its putative degradation products under stress degradation conditions. This information will be valuable for understanding the chemical stability of epalrestat, and developing suitable formulation and screening for appropriate storage conditions.

2. Experimental

2.1. Materials and reagents

The active pharmaceutical ingredient of epalrestat (purity > 99.5%) was obtained from Ningxia Kangya Pharmaceutical Industry (China). Acetonitrile and methanol of HPLC grade were purchased from Fisher (Fair lawn, NJ, USA). N,N-dimethyl formamide was obtained from Shandong Yuwang Industrial Co., Ltd (Shandong, China). Ammonium acetate (HPLC grade) was obtained from Dikma (Richmond Hill, NY, USA). Sodium dihydrogen phosphate, potassium phosphate monobasic and sodium phosphate dibasic dodecahydrate were purchased from Tianjin Kemiou Chemical Reagent Co., Ltd (Tianjin, China). Hydrochloric acid was obtained from Tianjin Kaixin Chemical Reagent Manufacturing Co., Ltd (Tianjin, China). H_2O_2 (30%), sodium hydroxide and sodium chloride were purchased from Tianjin Hengxing Chemical Reagent Manufacturing Co., Ltd (Tianjin, China). Ultra-pure water from Wahaha (Hangzhou, Zhejiang, China) was used. All other reagents and chemicals used were of analytical grade and are commercially available.

2.2. RP-HPLC conditions

Samples were analyzed on an HPLC system equipped with a 1110 pump, a 1310 column oven and a 1410 UV detector (HITACHI, Japan). Chromatographic separation was performed on a Waters C_{18} column (150 mm × 4.6 mm, 5 μm). The mobile phase consisted of acetonitrile buffer (25 mmol/L potassium phosphate monobasic and 25 mmol/L disodium hydrogen phosphate) at a ratio of 35:65 (v/v) and the pH was adjusted to pH 6.5 with phosphoric acid. The mobile phase was delivered at a flow rate of 1 mL/min and detection was performed with ultraviolet detection at 396 nm. Column temperature was maintained at 30 °C and the injection volume was 20 μL.

2.3. Sample preparation for degradation kinetic studies

A stock solution of epalrestat was prepared in *N*,*N*-dimethyl formamide at the concentration of 0.75 mg/mL. Epalrestat solutions were prepared using phosphate buffers of different pH values of 1.85, 3.13, 5.00, 7.10, 9.08 and 10.97 at 25 °C. The sample solutions were transferred into glass tubes and then incubated in a thermostat bath at predefined temperatures (25, 37, 60, 80 and 100 °C). To study the effects of ionic strength on the stability of epalrestat, sodium chloride was used to adjust ionic strength (0.3, 0.5, 0.7 and 0.9) while epalrestat solutions (150 μg/mL) were incubated at 25 and 60 °C. Three different concentrations of H_2O_2 (3%, 10% and 30%) were used and the epalrestat solutions were incubated at 25 °C to analyze the effect of oxidation on the stability of epalrestat. The sample solution for irradiation test was kept under the condition of daylight and compared with that shielded from light at 25 °C. Aliquots of the solution were removed periodically and rapidly cooled on ice to quench the reaction. The concentration for all the stability samples was 150 μg/mL. The samples were further diluted 10 times with methanol and filtered through a 0.22 μm membrane before analysis. The predetermined time points were designated as 0, 0.25, 0.5, 1.0, 2.0, 4.0, 6.0, 8.0, 12, and 24 h to analyze the effect of pH and ionic strength. Meanwhile, the predetermined time points were 0, 2, 5, 10, 20, and 30 min and 0, 0.083, 0.25, 0.5, 1, 1.5, 2, 3, and 4 h for testing the effect of oxidation and irradiation, respectively.

2.4. Identification of major degradation products

2.4.1. UHPLC-PDA-MS/MS conditions

A triple-quadrupole tandem mass spectrometer incorporating a Micromass® Quattro micro™ API mass spectrometer (Waters Corp., Milford, MA, USA) equipped with an electrospray ionization (ESI) interface was used for analytical detection. The chromatography was performed on an ACQUITY Ultra Performance LC™ system (Waters Corp., Milford, MA, USA) with a PDA detector. The separation was carried out on an ACQUITY™ UHPLC™ BEH C_{18} column (2.1 mm × 50 mm, 1.7 μm; Waters Corp., Milford, MA, USA). Gradient elution was applied using acetonitrile-5 mmol/L ammonium acetate as the mobile phase and programmed as follows: 0–1.0 min, 5% acetonitrile; 1.0–1.5 min, 26% acetonitrile (increased linearly); 1.5–13 min, 26% acetonitrile; and 13–15 min, 5% acetonitrile. The flow rate was set at 0.2 mL/min. The temperature of the column and autosampler were maintained at 30 °C and 4 °C, respectively, while the injection volume was 10 μL.

The ESI source was operated in negative ionization mode and the optimal MS parameters were capillary voltage set at 3.0 kV and cone voltage adjusted to 30 V. The source and desolvation temperatures were 120 °C and 450 °C, respectively. Nitrogen was used as the desolvation and cone gas at a flow rate of 500 and 30 L/h, respectively. Argon was employed as the collision gas while the optimized collision energy was 35 eV. Other mass spectrometry parameters were adopted according to the recommended values of the instrument. Full-scan MS data were collected from 50 to 400 Da.

2.4.2. Preparation of sample solutions

In the acidic and basic hydrolysis tests, 10 mg of epalrestat powder was precisely weighed and put into a 10 mL volumetric flask, then 2 mL of hydrochloric acid solution (1 mol/L) and sodium hydroxide solution (2 mol/L) were added. Hydrolysis was conducted at 40 °C for 12 h. In addition, the samples were cooled to room temperature and neutralized with sodium hydroxide solution (1 mol/L) and hydrochloric acid solution (2 mol/L). For the test of thermal degradation, epalrestat powder was heated on a gas lamp until they completely turned black. The epalrestat solutions were placed under the daylight conditions for 5 min and 2 mL of 10% H_2O_2 was used in the test of photolytic and oxidative degradation. The solutions obtained in the test above were diluted to 10 mL with *N*,*N*-dimethyl formamide. All the solutions were then diluted with methanol to the required concentration (100 μg/mL) and filtered through a 0.22 μm membrane. Finally, these solutions were kept in refrigerator at 4 °C before analysis by UHPLC-PDA-MS/MS. The blank samples for each stress condition were prepared without adding the analyte.

3. Results and discussion

3.1. Optimization of HPLC conditions

The composition of mobile phase was optimized to achieve satisfactory chromatographic behavior, such as good separation of epalrestat and other degradation products, appropriate analysis time and good peak shape. Acetonitrile was selected as the organic phase since it provided a better peak shape compared with

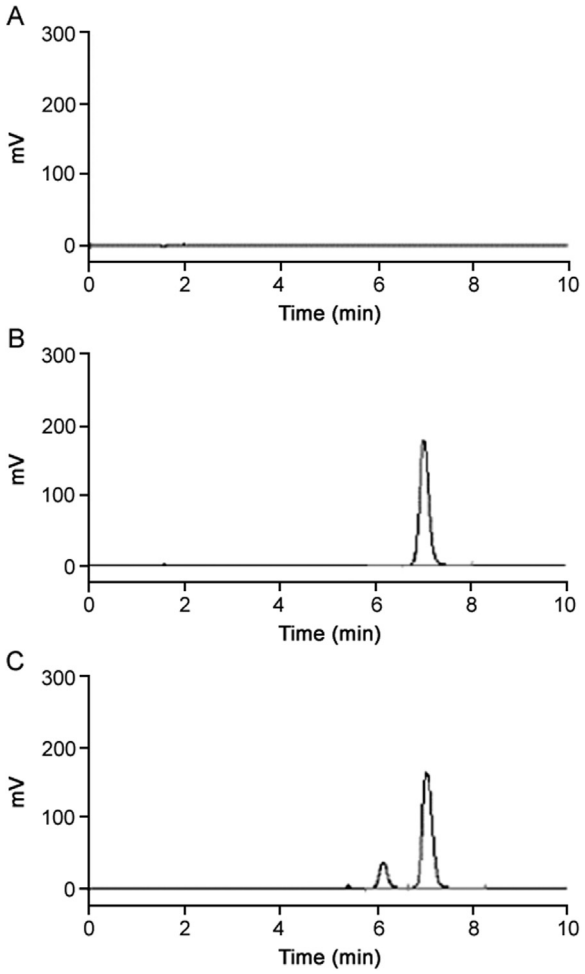

Fig. 1. Typical chromatograms of (A) blank solution, (B) blank solution spiked with epalrestat (15 μg/mL) and (C) a sample after 10 min under the condition of daylight.

methanol. However, when acetonitrile-water was selected as the mobile phase, a poor peak shape was observed. We therefore investigated the effect of different concentrations of phosphate buffer salt on peak shape and found that the ideal peak shape was achieved with 25 mmol/L potassium phosphate monobasic and 25 mmol/L disodium hydrogen phosphate in water. The pH of epalrestat aqueous solution was also studied. A more symmetric peak shape and better separation of epalrestat and other degradation products were achieved with the pH value of the mobile phase adjusted to 6.5. Moreover, to achieve appropriate analysis time, the organic-to-aqueous ratio in the mobile phase was also tested and a ratio of 35:65 (v/v) was selected. Consequently, a mobile phase with pH 6.5 consisting of an acetonitrile buffer solution (35:65,v/v) was chosen (buffer solution: 25 mmol/L potassium phosphate monobasic and 25 mmol/L disodium hydrogen phosphate in water).

3.2. Optimization of UHPLC-PDA-MS/MS conditions

The effects of mobile phase combinations on the response of epalrestat and degradation products along with peak shape were investigated. Compared to methanol, acetonitrile was found to achieve a higher response. In addition, it was found that the sensitivity and peak shape of epalrestat and its degradation products were both improved when ammonium acetate was added to the mobile phase. Consequently, the effect of adding different concentrations (5 mmol/L, 10 mmol/L) of ammonium acetate into the mobile phase was investigated and 5 mmol/L ammonium acetate was found to be beneficial for monitoring higher abundance of epalrestat and its degradation products as well as achieving a better peak shape of the analytes. To achieve adequate separation of the analytes, a gradient elution was also employed in the experiment.

To attain the most sensitive ionization method for the degradation products of epalrestat, both positive and negative ion modes were tested and it was found that the highest signal intensity and optimal response were obtained with the negative ion modes. Moreover, in the process of multiple reaction monitoring (MRM), a higher signal intensity was also obtained for their products in the negative mode. Other mass spectrometry parameters were also optimized to achieve better responses to all analytes.

3.3. Method validation

Methods pertaining to selectivity, repeatability, linearity, precision and accuracy were also validated. A good peak shape was achieved under the described conditions without interference from other degradation products. The typical chromatograms of epalrestat and degraded sample are shown in Fig. 1. A linear calibration curve for epalrestat was obtained over the range of 0.5–24.0 μg/mL while the typical equation calibration curve was $A = 1.6 \times 10^5\ C – 1.3 \times 10^3$ ($r = 0.999$), where A represents the peak area of epalrestat and C is the concentration of epalrestat. The results of intra-day and inter-day precision, accuracy and repeatability all met their respective requirements and are shown in Table 1.

3.4. Kinetic calculations of rate constant (k) and half-life ($t_{1/2}$)

In our experiment, the reaction order of the degradation of epalrestat was determined by plotting concentration or $\ln(C_t/C_0)$ versus time under different degradation conditions. The plot of $\ln(C_t/C_0)$ against time showed a strong correlation and the results indicated that the degradation of epalrestat followed the first-order rate kinetics. The observed degradation rate constants (k) were calculated from first-order plots based on the following equation (E_1):

$$\ln \frac{C_t}{C_0} = -kt \quad \text{(E1)}$$

where C_0 is the initial concentration, C_t is the time-dependent concentration, and t is the time. Moreover, the first-order plots under all experimental conditions yielded a correlation coefficient greater than 0.9.

The half-life ($t_{1/2}$) of the test drug was calculated as (E_2):

$$t_{1/2} = \ln 2/k \quad \text{(E2)}$$

Table 1
The results of accuracy, precision and repeatability in the method validation.

Parameter	Concentration (μg/mL)	Recovery (%)	RSD (%)
Accuracy	1.00	99.6 ± 0.87	1.0
	6.00	98.5 ± 0.22	
	20.00	98.6 ± 1.1	
Precision	6.00		1.1
Repeatability	6.00		0.9

Table 2
Rate constant (k) and half-time ($t_{1/2}$) of epalrestat at different pH and temperatures (T).

pH	Parameters	T (°C)				
		25	37	60	80	100
1.85	$k(h^{-1})$	0.0160	0.0206	0.0234	0.0282	0.0655
	$t_{1/2}$(h)	43.31	33.64	29.62	24.57	10.58
3.13	$k(h^{-1})$	0.0159	0.0194	0.0206	0.0297	0.0627
	$t_{1/2}$(h)	43.58	35.72	33.64	23.33	11.05
5.00	$k(h^{-1})$	0.0060	0.0115	0.0191	0.0302	0.0717
	$t_{1/2}$(h)	115.5	60.26	36.28	22.95	9.67
7.10	$k(h^{-1})$	0.0043	0.0153	0.0195	0.0280	0.0695
	$t_{1/2}$(h)	161.16	45.29	35.54	24.75	9.97
9.08	$k(h^{-1})$	0.0033	0.0122	0.0194	0.0264	0.0690
	$t_{1/2}$(h)	210.00	56.80	35.72	26.25	10.04
10.97	$k(h^{-1})$	0.0016	0.0036	0.0140	0.0267	0.0724
	$t_{1/2}$(h)	433.12	192.5	49.5	25.96	9.57

3.5. Analysis of degradation kinetics

3.5.1. The influence of pH on the stability of epalrestat

The degradation rate constant (k) and half-life ($t_{1/2}$) at different pH values from 25 °C to 100 °C were calculated and are listed in Table 2. The stability of epalrestat at 25 °C in various pH solutions is shown in Fig. 2A. As can be seen, the degradation rate constant of epalrestat decreased with increased pH, demonstrating that the maximum stability was obtained at approximately pH 10.97. When pH was < 3.13, the rate of degradation was rapid, while at pH > 5.00, the rate of degradation decreased with increased pH. These results showed that the degradation of epalrestat was pH-dependent, and epalrestat was more stable under alkaline than acidic conditions which may indicate that there is general acid catalysis in the decomposition reactions.

3.5.2. The influence of temperature on the stability of epalrestat

The temperature (T) dependence of epalrestat degradation at different pH values was investigated in the temperature range of 25–100 °C. The relevant equations related to the influence of temperature on the degradation of epalrestat are as follows:

The activation energy (Ea) was calculated as the Arrhenius equation (E_3) [33]:

$$\ln k = \ln A - \frac{E_a}{RT} \quad \text{(E3)}$$

where A is the Arrhenius factor, Ea is the activation energy (kJ/mol). R is the universal gas constant (8.314 J/K/mol), and T is the absolute temperature (K).

The shelf-life ($t_{0.9}$), enthalpy of activation ($\triangle H^{\ddagger}$) and entropy of activation ($\triangle S^{\ddagger}$) were calculated as follows:

$$t_{0.9} = \frac{0.1054}{k} \quad \text{(E4)}$$

$$\Delta H^{\ddagger} = E_a - RT \quad \text{(E5)}$$

$$\Delta S^{\ddagger} = \frac{\Delta H^{\ddagger}}{T} - R \ln \frac{T}{k'} - R \ln \frac{k'}{h} \quad \text{(E6)}$$

where k' and h are the Boltzmann constant of 1.3807×10^{-23} J s and the Planck's constant of 6.626×10^{-34} J s, respectively.

The Arrhenius relationship plotting ln k versus $1/T$ at various pH values and the kinetic parameters were all calculated and are listed in Table 3. The results show that the ln k was linear ($r > 0.9$) with the reciprocal of absolute temperature ($1/T$) in the temperature range of 25–100 °C. Table 3 also shows that k increased with rised T at selected pH values, indicating that the degradation of epalrestat was accelerated by the increase in temperature. It was also found that the slope of the Arrhenius equation (Ea/R) was greater and epalrestat was more stable at high pH values, which was consistent with the effect of pH on the stability of epalrestat. Moreover, when at a selected pH value, for instance, the $t_{0.9}$ at 25, 37, 60, 80 and 100 °C was 65.88, 29.28, 7.53, 3.95 and 1.46 at the pH of 10. 97, which suggests that the $t_{0.9}$ was decreased with increased temperature.

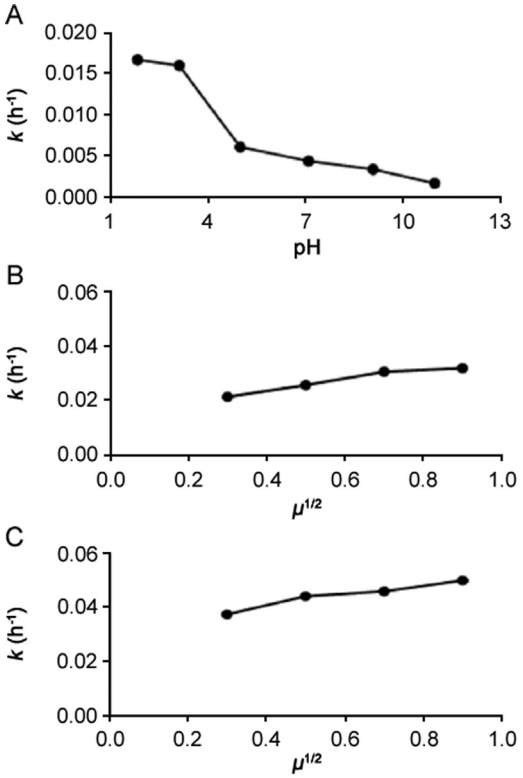

Fig. 2. (A) Relationship between rate constant (k) and pH in various pH solutions at 25 °C, the influence of ionic strength on the stability of epalrestat at (B) 25 °C and (C) 60 °C.

3.5.3. The influence of ionic strength on the stability of epalrestat

The influence of ionic strength (μ) on the stability of drugs may be described by the following Debye–Huckel equation (E_7) [34]:

$$\log k = \log k_0 + 1.022 Z_A Z_B \sqrt{\mu} \quad \text{(E7)}$$

where k_0 is the rate constant when ionic strength is zero ($\mu = 0$), Z_A and Z_B represent the charges of the drug solution and competing ion, respectively.

The influence of ionic strength was determined at fixed temperature (25 °C and 60 °C). As shown in Fig. 2B and Fig. 2C, the degradation rate constant of epalrestat increased with increased ionic strength, from 0.3 to 0.9 M at 25 °C. These results illustrate that the ionic reactions are present in the degradation process of epalrestat and that adding a salt to the solution has a negative effect on the stability of epalrestat. The slope of the line was 1.10, 1.06, 0.94 and 0.96, which was in agreement with the expected value (1.022) obtained from the above equation (E_7). Additionally, temperature also affects the effect of ionic strength on the degradation rate constant and with the increase in ionic strength, the obtained degradation rate constant of epalrestat was higher at 60 °C than at 25 °C.

3.5.4. The influence of oxidation on the stability of epalrestat

The influence of oxidation on the stability of epalrestat was investigated using three different concentrations of H_2O_2 (3%, 10%

Table 3
Arrhenius relationship and activation parameters of epalrestat in various pH solutions.

pH	activation	r	E_a(kJ/mol)	$\triangle H^{\ddagger}$(kJ/mol)	$\triangle S^{\ddagger}$(J/K/mol)
1.85	$\ln k = -1745.5\ (1/T) + 1.7$	0.9072	14.51	11.74	−647.95
3.13	$\ln k = -1785.9\ (1/T) + 1.7$	0.9098	14.85	12.07	−646.94
5.00	$\ln k = -3367.9\ (1/T) + 6.2$	0.9861	28.00	25.23	−607.24
7.10	$\ln k = -3462.2\ (1/T) + 6.5$	0.9454	28.78	26.01	−604.87
9.08	$\ln k = -3862.4\ (1/T) + 7.6$	0.9563	32.11	29.34	−594.83
10.97	$\ln k = -5554.5\ (1/T) + 12.3$	0.9973	46.18	43.41	−552.37

and 30%). The plots of $\ln(C_t/C_0)$ versus time at various concentrations of H_2O_2 are shown in Fig. 3A. The degradation rate constant (k) were −0.32, −0.56 and −3.9 in 3%, 10% and 30% H_2O_2 solutions, respectively. These results demonstrated that epalrestat was extremely unstable under oxidation conditions since the degradation rate constant increased noticeably with increased concentration of H_2O_2. These results suggest that epalrestat solution should be stored in an anoxic environment.

3.5.5. *The influence of irradiation on the stability of epalrestat*

Epalrestat powder gradually fades in color and decomposes on exposure to light [35]. Epalrestat solution also decomposed under the same condition. To confirm the degradation rate of epalrestat, a sample was kept under indirect daylight at room temperature. The plot of concentration versus time showed that the content of epalrestat was only a third of that protected from light after 15 min. $\mathrm{Ln}(C_t/C_0)$ versus time under indirect daylight was plotted as shown in Fig. 3B, The results showed that the content of epalrestat remained constant after 15 min, which suggests that epalrestat and its isomers can interconvert and the content maintains a certain proportionality when epalrestat is partially degraded. These results demonstrated that epalrestat solution should be stored away from light.

3.6. *Characterization of the major degradation products*

Stress degradation studies of epalrestat were performed under different stress conditions (acidic, alkaline, thermal, oxidation, and irradiation). UHPLC-PDA-MS/MS chromatograms of epalrestat degraded solutions were compared with standard solutions of epalrestat, as well as with the similarly treated blank solutions, to identify peaks of the degradation products. A tentative assignment of the degradation products was made on the basis of parent ion $[M\text{-}H]^-$ and fragment ions obtained from UHPLC-PDA-MS/MS experiments. Some peaks were not detected by UHPLC-PDA-MS/MS possibly due to poor ionizability or low concentration of the degradation products.

The typical $[M\text{-}H]^-$ ion of the degradation product in acidic media was m/z 175.1, which suggested that its molecular weight was 176, there was no nitrogen atom in the molecular structure of this degradation product, and the MS^2 spectra of the degradation products exhibited the product ions at m/z 58.8. Meanwhile alpha-methylcinnamaldehyde ($C_{10}H_{10}O$) was one of the materials from the synthesis process of epalrestat and accordingly the degradation product could be unambiguously confirmed as $C_{12}H_{16}O$ (DP1: Degradation Product 1) and the product ions was $C_3H_7O^-$. The degradation product was observed under alkaline condition with a typical $[M\text{-}H]^-$ ion at m/z 115.8. Its molecular weight was suggested to be 117, and a nitrogen atom was included in the molecular structure. The MS^2 spectra of the degradation product exhibited the product ion at m/z 57.8, suggesting that its molecular formula was C_4H_7NOS (DP2) and the product ions was CNS^-. The thermal degradation product was observed with typical $[M\text{-}H]^-$ ion at m/z 190.1 and the MS^2 spectra of the degradation product exhibited the product ion at m/z 57.8, indicating that its molecular formula was $C_5H_5NO_3S_2$ (DP3). Under oxidation conditions the degradation product was observed with the typical $[M\text{-}H]^-$ ion at m/z 198.1, and the MS^2 spectra of the degradation products exhibited the product ions at m/z 57.8 and 99.9. This demonstrated that the molecular formula was $C_8H_9NOS_2$ (DP4), and the product ion was $C_3H_2NOS^-$ when the m/z was 99.9. The MRM chromatograms (A, C, E, and G), product ion spectra (B, D, F, and H) and the proposed structures of the degradation products of epalrsetat in acidic, alkaline, thermal and oxidation conditions are shown in Fig. 4.

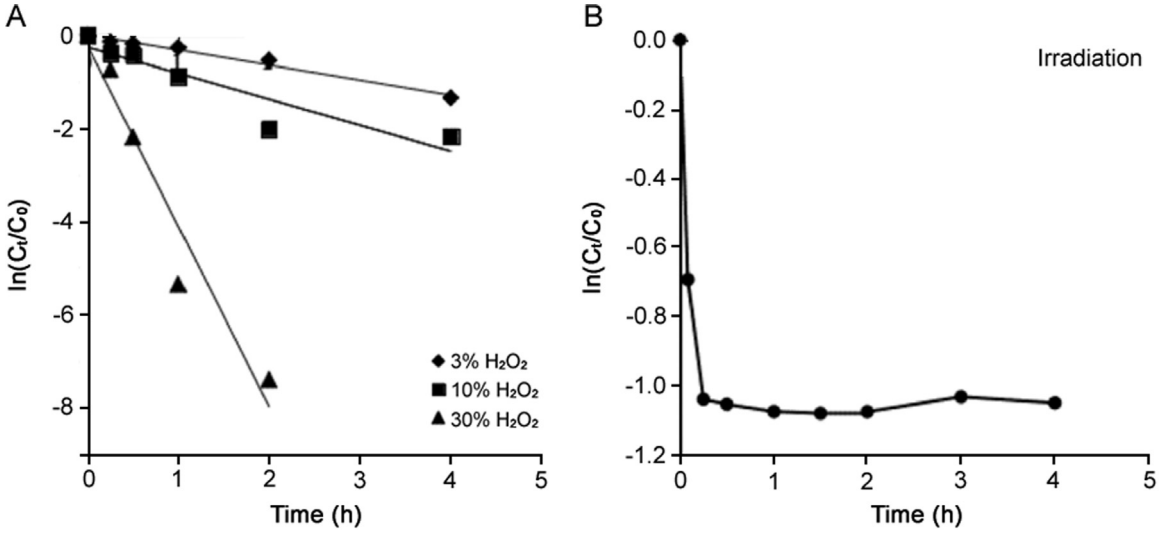

Fig. 3. $\ln(C_t/C_0)$ versus time (A) at various concentrations of H_2O_2, and (B) under indirect daylight.

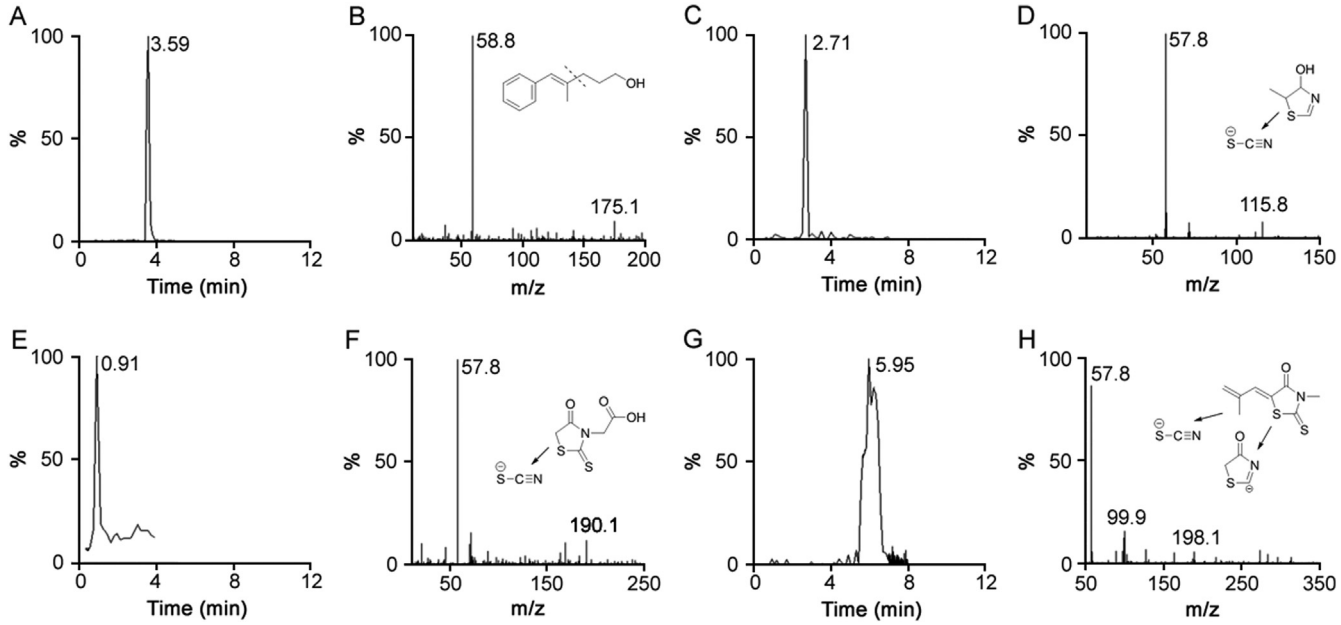

Fig. 4. MRM chromatograms (left column), product ion spectra (right column) and proposed structures of the degradation products of epalrsetat in acidic, alkaline, thermal and oxidation conditions. (A) DP1 (acidic), (B) DP1 (acidic), (C) DP2 (alkaline), (D) DP2 (alkaline), (E) DP3 (thermal), (F) DP3 (thermal), (G) DP4 (oxidation), and (H) DP4 (oxidation).

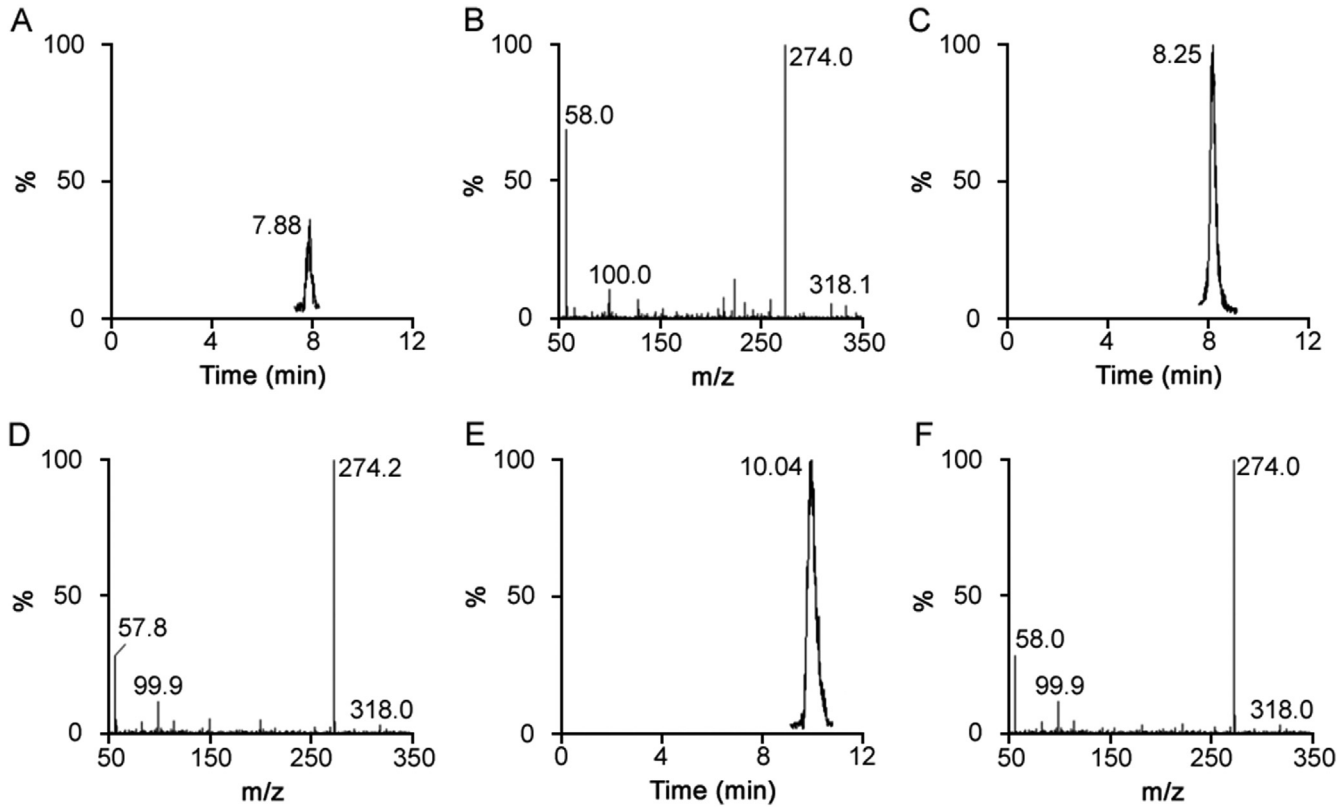

Fig. 5. (A, C, and E) MRM chromatograms and (B, D, and F) product ion spectra of the three degradation products of epalrsetat under the irradiation condition.

Three peaks were detected in the irradiation condition by comparing the retention time with that of standard compounds. The parent ions of the three degradation products were identical and the $[M\text{-}H]^-$ was 318. The product ions were also identical (*m/z* were 274, 100 and 58). The parent ions and the product ions of the three degradation products were all consistent with those of epalrestat. The results could also be surmised from the structure of epalrestat, which contains a conjugated dienes structure with four geometric isomers. Consequently the three degradation products are likely to be the isomers of epalrestat. The MRM

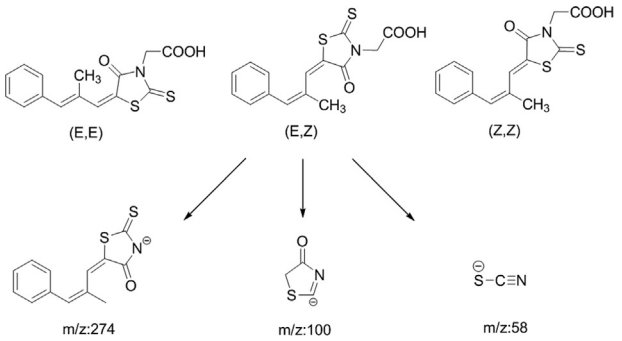

Fig. 6. Structures of the three degradation products and the proposed ESI-MS/MS fragmentation pathways of the three degradation products (taking an example of the *(E,Z)* structure).

chromatograms and product ion spectra of the degradation products of epalrestat under the irradiation condition are shown in Fig. 5. The structures of the three degradation products are shown in Fig. 6, but the three degradation products which may be the isomers can not be identified solely by mass spectrometry. For example, the structure of (*E,Z*), the proposed ESI-MS/MS fragmentation pathways of the three degradation products are also shown in Fig. 6 and it can be seen that the product ions from Fig. 5 and Fig. 6 are consistent with those of previous reports [24].

4. Conclusion

In the present study, an UHPLC-PDA-MS/MS method was established and validated. It was used for the determination of epalrestat and analysis of degradation kinetics of epalrestat in aqueous solution. The results indicated that the pH, temperature, ionic strength, oxidation and irradiation greatly influence the stability of epalrestat and the degradation behavior of epalrestat followed first-order kinetics. Epalrestat was most stable in neutral, alkaline, lower temperature conditions and lower ionic strength. Epalrestat would be extremely unstable under conditions of oxidation and irradiation. Investigating of suitable storage conditions for epalrestat should consider the influence of pH, temperature, ionic strength, oxidation and irradiation.

In this study, the degradation products of epalrestat were analyzed by subjecting the compound to various stress degradation conditions recommended by ICH for the first time. A total of seven degradation products were detected and four degradation products were tentatively identified by analyzing the mass fragmentation patterns of epalrestat and mass analysis of the degradation products. This study was a typical example of the development of a stability-indicating assay established following the recommendations of ICH guidelines. The information obtained from the degradation kinetics will be helpful for understanding the stability of epalrestat and providing a reference for further studies of epalrestat clinic applications.

Conflicts of interest

The authors declare that there are no conflicts of interest.

References

[1] X. Li, Y. Shen, Y. Lu, et al., Amelioration of bleomycin-induced pulmonary fibrosis of rats by an aldose reductase inhibitor, epalrestat, Korean J. Physiol. Pharmacol. 19 (2015) 401–411.
[2] T. Kawai, I. Takei, M. Tokui, et al., Effects of epalrestat, an aldose reductase inhibitor, on diabetic peripheral neuropathy in patients with type 2 diabetes, in relation to suppression of Nε-carboxymethyl lysine, J. Diabetes Complicat. 24 (2010) 424–432.
[3] N. Hotta, R. Kawamori, M. Fukuda, et al., Long-term clinical effects of epalrestat, an aldose reductase inhibitor, on progression of diabetic neuropathy and other microvascular complications: multivariate epidemiological analysis based on patient background factors and severity of diabetic neuropathy, Diabet. Med. 29 (2012) 1529–1533.
[4] R. Nirogi, V. Kandikere, D.R. Ajjala, et al., LC-MS/MS method for the quantification of aldose reductase inhibitor-Epalrestat and application to pharmacokinetic study, J. Pharm. Biomed. Anal. 74 (2013) 227–234.
[5] A. Ito, R. Ishii-Nozawa, C. Ibuki, et al., Examination of questionnaires items regarding diabetic peripheral neuropathy in epalrestat-treated patients and their usefulness in the treatment of this disorder-influence on treatment course, Yakugaku. Zasshi. 129 (2009) 1239–1247.
[6] L.X. Ji, N. Shen, C.N. Li, et al., Inhibition effect of eplrestat on rat lens osmotic expansion, Acta Pharm. Sin. 44 (2009) 1107–1111.
[7] G. Hou, R. Zhang, Z. Pi, et al., A new method for screening aldose reductase inhibitors using ultrahigh performance liquid chromatography-tandem mass spectrometry, Anal. Methods 6 (2014) 7681–7688.
[8] F. Azpiroz1, C. Malagelada, Diabetic neuropathy in the gut: pathogenesis and diagnosis, Diabetologia 59 (2016) 404–408.
[9] K. Ozaki, H. Hamano, T. Matsuura, et al., Effect of deoxycorticosterone acetate-salt-induced hypertension on diabetic peripheral neuropathy in alloxan-induced diabetic WBN/Kob rats, J. Toxicol. Pathol. 29 (2016) 1–6.
[10] P. Hewston, N. Deshpande, Falls and balance impairments in older adults with type 2 diabetes: thinking beyond diabetic peripheral neuropathy, Can. J. Diabetes 40 (2016) 6–9.
[11] K. Sato, K. Yama, Y. Murao, et al., Epalrestat increases intracellular glutathione levels in Schwann cells through transcription regulation, Redox Biol. 2 (2014) 15–21.
[12] H. Ando, T. Takamura, Y. Nagai, et al., Erythrocyte sorbitol level as a predictor of the efficacy of epalrestat treatment for diabetic peripheral polyneuropathy, J. Diabetes Complicat. 20 (2006) 367–370.
[13] H. Wang, Y.L. Ma, Epalrestat diabetic peripheral clinical efficacy and safety studies neuropathy treatment, Diabetes New World 9 (2016) 35–36.
[14] J.Q. Ma, Analysis of effect on epalrestat adjunctive treatment to the patients with diabetic peripheral neuropathy, China Contin. Med. Educ. 7 (2015) 221–222.
[15] Y. Goto, N. Hotta, Y. Shigeta, et al., Effects of an aldose reductase inhibitor, epalrestat, on diabetic neuropathy, Clinical benefit and indication for the drug assessed from the results of a placebo-controlled double-blind study, Biomed. Pharmacother. 49 (1995) 269–277.
[16] N. Hotta, N. Sakamoto, Y. Shigeta, et al., Clinical investigation of epalrestat, an aldose reductase inhibitor, on diabetic neuropathy in Japan: multicenter study, J. Diabetes Complicat. 10 (1996) 168–172.
[17] N. Hotta, R. Kawamori, Y. Atsumit, et al., Stratified analyses for selecting appropriate target patients with diabetic peripheral neuropathy for long-term treatment with an aldose reductase inhibitor, epalrestat, Diabet. Med. 25 (2010) 818–825.
[18] K. Matsuoka, N. Sakamoto, Y. Akanuma, et al., A long-term effect of epalrestat on motor conduction velocity of diabetic patients: ari-diabetes Complications Trial (ADCT), Diabetes Res. Clin. Pract. 77 (2007) S263–S268.
[19] T. Li, H. Wang, Z. Zheng, Assay of epalrestat tablets and its test for related substances by HPLC, Drug Stand. China 2 (2015) 109–111.
[20] Y.B. Ma, R.M. Li, B. Ren, et al., Determination of the related substances in epalrestat tablets by RP -HPLC, China Pharm. 19 (2008) 1736–1737.
[21] S. Seelam, K. Dhanalakshmi, G.N. Reddy, Validation of derivative spectrophotometric and UPLC methods for quantitative determination of epalrestat in bulk and pharmaceutical dosage form, Int. J. Clin. Pharm. Net 5 (2013) 341–346.
[22] A.A. Shirkhedkar, C.S. Nankar, S.J. Surana, Quantitative determination of epalrestat by RP-HPLC method, Eurasia. J. Anal. Chem. 7 (2012) 49–55.
[23] M.L. Qi, P. Wang, J.J. Yang, Determination of stereoisomers of epalrestat by liquid chromatography, J. Beijing Inst. Technol. 13 (2004) 445–448.
[24] H. Sun, Y. Bo, M. Zhang, et al., Simultaneous determination of epalrestat and puerarin in rat plasma by UHPLC-MS/MS: application to their pharmacokinetic interaction study, Biomed. Chromatogr. 31 (2017) e3855.
[25] Y.F. Xie, C.Y. Chen, Z.X. Rong, et al., HPLC determination of plasma epalrestat and its pharmacokinetics in Chinese healthy subjects, Acta Univers. Med. Secon. Shanghai 6 (2003) 502–504.
[26] Z.C. Yu, S. Lu, Y.D. Shao, et al., Determination of epalrestat in human plasma by high performance liquid chromatography and its pharmacokinetics, Chin. Pharm. J. 3 (2000) 42–44.
[27] Z.C. Yu, W.H. Yang, C.Y. Liu, et al., Pharmacokinetics of epalrestat after a single and multiple oral dose in healthy volunteers, Chin. J. Clin. Pharmacol. 3 (2000) 205–208.
[28] M.N. Sarat, P.G. Birajdar, P. Loya, et al., Rapid and sensitive HPTLC method for determination of epalrestat in human plasma, JPC J. Planar Chromatogr. 20 (2007) 203–207.
[29] C. Wang, W. Chang, Drugs would be intravenous injection protected from light, Chin. Pharm. Aff. 22 (2008) 77–79.
[30] M. Caianelo, C. Rodrigues-Silva, M.G. Maniero, et al., Antimicrobial activity against Gram-positive and Gram-negative bacteria during gatifloxacin degradation by hydroxyl radicals, Environ. Sci. Pollut. Res. Int. 24 (2017) 6288–6298.

[31] S.C. Shim, A.N. Pae, Y.J. Lee, Mechanistic studies on the photochemical degradation of nifedipine, Bull. Korean Chem. Soc. 9 (1988) 271–274.
[32] T. Handa, S. ingh, I.P. Singh, Characterization of a new degradation product of nifedipine formed on catalysis by atenolol: a typical case of alteration of degradation pathway of one drug by another, J. Pharm. Biomed. 89 (2014) 6–17.
[33] J.O. Fubara, R.E. Notari, Influence of pH, temperature and buffers on cefepime degradation kinetics and stability predictions in aqueous solutions, J. Pharm. Sci. 87 (2010) 1572–1576.
[34] X.W. Teng, D.C. Cutler, N.M. Davies, Degradation kinetics of mometasone-furoate in aqueous systems, Int. J. Pharm. 259 (2003) 129–141.
[35] Japanese Pharmacopoeia, Seventeenth Edition (JP17). Supplement I, 2016: 865-866.